Nonequilibrium transitions in driven AB_3 compounds on the fcc lattice: A multivariate master-equation approach

F. Haider*
Institut für Metallphysik, University of Göttingen, Hospitalstrasse 3/5, D-3400 Göttingen, West Germany

P. Bellon and G. Martin
Section de Recherches de Métallurgie Physique, Centre d'Etudes et de Recherches sur les Materiaux, Centre d'Etudes Nucléaires de Saclay, F-91191 Gif-sur-Yvette CEDEX, France
(Received 4 April 1990)

We studied the order-disorder transition in an Ising-type alloy on a fcc lattice with AB_3 stoichiometry with atomic exchanges due to two competing processes: thermally activated jumps and ballistic jumps, as, for example, is the case under irradiation with high-energy particles. The latter favor disordered configurations, while the former tend to restore a certain degree of order. The state of order is described by a four-dimensional parameter, the occupation of the four simple cubic sublattices into which the fcc lattice may be decomposed. In a mean-field approximation the kinetic equations for the evolution of this order parameter can be found. For a stochastic description, the master equation for the probability of a given state of order is approximated using Kubo's ansatz. The resulting partial differential equation is solved taking advantage of symmetry properties of the order-parameter space. A dynamical-equilibrium phase diagram is constructed, and it is shown that new phases, not found under thermal conditions, can be stabilized for a certain model for the saddle-point energy of the thermal jumps.

I. INTRODUCTION

Nonequilibrium phase transitions, i.e., transitions between steady states of a dynamical system, rather than between equilibrium states of a thermodynamical system, are of interest in a large variety of fields. In materials science, one example is given by radiation-induced phase transitions.[1] The latter occur when atoms are ejected from their equilibrium position by nuclear collisions. The configuration of the system results, in most simple examples, from a competition between radiation-induced disorder due to atomic jumps induced by nuclear collisions ("ballistic jumps") and thermally activated reordering due to the usual atomic jumps (thermal jumps of point defects). One may say that the configuration space of such systems is explored following two dynamics that act in parallel: the usual thermal jumps, which favor the occupancy of low-energy configurations, and the ballistic jumps that occur irrespective of the value of the energy of the configuration. Under the effect of ballistic jumps only, the configuration space is explored as it would be at infinite temperature. In previous works,[2-4] we studied the order-disorder transition on a rigid lattice for some structures which could be described by a scalar order parameter: the steady-state probability of a given degree of order in the system assumed to be spatially uniform could be found as the solution of a simple master equation, built in such a way as to reproduce the thermal equilibrium probability in the absence of ballistic jumps. We treated both the case of single-step processes (i.e., where pairs exchange between the sublattices one at a time) and multistep processes (i.e., where several pairs exchange at once as is the case in collision cascades). In the latter case, the master equation was approximated by a Fokker-Planck equation.

The problem of handling crystallographic structures with more than two Wyckoff positions, i.e., for which the degree of order is described by more than one free parameter at a given overall concentration, remained open. Here we address this question, starting with a relatively simple case: The face-centered-cubic lattice with AB_3 stoichiometry. Indeed the fcc structure can be described with four simple-cubic sublattices. Setting the composition of each sublattice gives the description of the simplest superstructures (e.g. $L1_2$ and $L1_0$). As before, we restrict to spatially homogeneous systems; moreover, here we handle only single-step processes, i.e., *single atomic pair exchanges* between nearest-neighbor sites driven both by thermal and ballistic jumps. This is an idealization of high-energy electron irradiations. When handling multidimensional order parameters, two difficulties arise: (1) in the thermal case the Fokker-Planck equation is a bad approximation of the master equation, detailed balance of the latter does not guarantee zero probability flux in the Fokker-Planck equation, and (2) in the driven case (i.e., when ballistic jumps occur in parallel to thermal jumps) detailed balance does not hold any more. The above two problems can be overcome using a technique introduced by Kubo.[5]

In the following we first recall the mean-field thermodynamics of the thermal model, then introduce the kinetic description of the model, compatible with the thermo-

dynamics. The stochastic description is introduced in Sec. IV as well as Kubo's ansatz. A nonlinear partial differential equation results for the potential. We show in Sec. V how the latter can be solved by taking advantage of the symmetry properties of the order-parameter space. The dynamical equilibrium phase diagram for AB_3 compounds is deduced and exhibits unexpected features.

II. THE MODEL—THERMODYNAMICS

The simplest ordered structures of a binary alloy on the fcc-lattice of composition AB_3, i.e., $L1_2$ and $L1_0$, can be described by the average A occupation of the simple cubic sublattices, into which the fcc-lattice can be decomposed (see Fig. 1). Using the vector $\mathbf{X}$ of concentrations x_i of A atoms on sublattice i,

$$x_i=\frac{A_i}{\Omega}, \quad i=1,\ldots,4 \tag{1}$$

(Ω is the number of sites per sublattice), as four-dimensional order parameter, the free energy in a Bragg-Williams approximation reads[6]

$$\begin{aligned} F(\mathbf{X})&=F_0-\Omega kT\sum_{i=1}^{4} f(x_i) , \\ f(x)&=2\frac{\omega}{kT}x^2-[x\ln x+(1-x)\ln(1-x)] , \\ \omega&=v_{AA}+v_{BB}-2v_{AB} , \end{aligned} \tag{2}$$

where v_{ij} is the contribution on an ij pair to the ordering energy.

The stable or metastable states, the minima of F under the constraint

$$\sum_{i=1}^{4} x_i=1 , \tag{3}$$

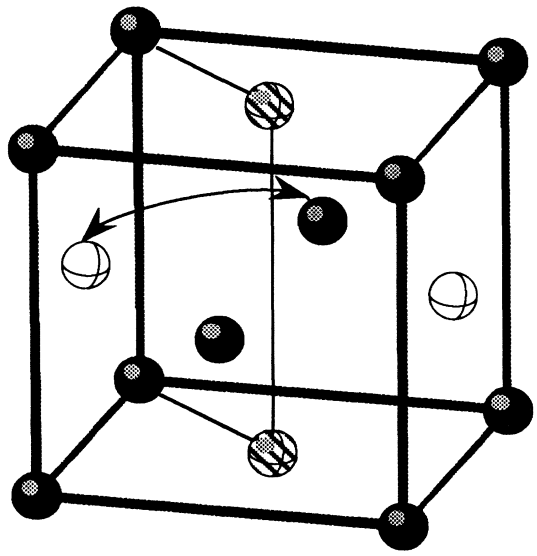

FIG. 1. Unit cell of the fcc lattice showing the four sublattices and the exchange of two neighboring atoms through the "saddle-point window" formed by four atoms.

are given as solution of

$$4\frac{\omega}{kT}(x_i-\tfrac{1}{4})-\ln\frac{x_i}{1-x_i}=\tfrac{1}{4}\sum_{j=1}^{4}\ln\frac{x_j}{1-x_j} , \quad i=1,\ldots,4 . \tag{4}$$

III. KINETIC DESCRIPTION

The stable thermodynamic states can be regarded as well as the infinite-time solutions of an equivalent kinetic model. Such a kinetic description facilitates the extension to externally driven systems like radiation-induced disordering. To construct a kinetic model, we suppose as elementary step the exchange of an A atom on sublattice i with a B atom on sublattice k, i.e., a change

$$\begin{aligned} &x_i\rightarrow x_i-\frac{1}{\Omega} \\ &\text{and} \\ &x_k\rightarrow x_k+\frac{1}{\Omega} \end{aligned} \tag{5}$$

in vector notation

$$\mathbf{X}\rightarrow\mathbf{X}+\boldsymbol{\epsilon}_{ik}, \quad (\boldsymbol{\epsilon}_{ik})_j=\frac{1}{\Omega}(\delta_{kj}-\delta_{ij}) . \tag{6}$$

Then the kinetic equations can be written as

$$\frac{\partial}{\partial t}x_i=\sum_{k=1}^{4}[w(\mathbf{X}\rightarrow\mathbf{X}+\boldsymbol{\epsilon}_{ki})-w(\mathbf{X}\rightarrow\mathbf{X}+\boldsymbol{\epsilon}_{ik})] . \tag{7}$$

$w(\mathbf{X}\rightarrow\mathbf{x}+\boldsymbol{\epsilon}_{ki})$ is the rate of transitions from $\mathbf{X}$ to $\mathbf{X}+\boldsymbol{\epsilon}_{ik}$, that is the number of AB exchanges between sublattices i and k per unit time, divided by the number of sites per sublattice Ω. Under the same assumptions as made for the thermodynamic model, i.e., mean-field-approximation and bond counting, we can construct the $w(\mathbf{X}\rightarrow\mathbf{X}+\boldsymbol{\epsilon}_{ik})$ as the product of the rate of atomic exchanges between sublattices i and k, $\Gamma_{ik}(\mathbf{X})$, multiplied by the probability to find an A atom on sublattice i and a nearest-neighbor B atom on sublattice k: in mean-field approximation

$$w(\mathbf{X}\rightarrow\mathbf{X}+\boldsymbol{\epsilon}_{ki})=\frac{z}{3}x_i(1-x_k)\Gamma_{ik}(\mathbf{X}) , \tag{8}$$

where $z=12$ is the coordination number of the fcc lattice, $z/3$ is the number of links between one site on sublattice i and the next-neighbor sites on sublattice k.

The thermal jump frequency Γ_{ik}^{th} is proportional to the exponential of the energy necessary to lift an A and a B atom into the saddle-point position, divided by kT:

$$\Gamma_{ik}^{\text{th}}(\mathbf{X})=\Gamma_0\exp\left[-\frac{1}{kT}E_a(\mathbf{X})\right] . \tag{9}$$

For the activation barrier E_a, we take the following model: E_a is the energy required to remove an A atom from sublattice i and a B atom from sublattice k and to lift them to the saddle-point position; the latter includes a constant term E_0 and a "chemical contribution" estimated by counting the bonds between the atom at the saddle

point and the four atoms surrounding the saddle point[7] (cf. Fig. 1):

$$E_a(\mathbf{X})=\frac{z}{6}\omega(x_i-x_k)+2\omega_0(1-x_i-x_k)+2E_0 \qquad (10)$$

with

$$\omega_0=(v^*_{AA}-v_{AA})-(v^*_{BB}-v_{BB}) ,$$

where v^*_{ij} denotes the binding energy of an atom of type i in the saddle point with one of type j in the lattice.

According to the model, the parameter ω_0 is thus related to the difference in activation energies for self-diffusion in each pure material, A, respectively, B. As can be seen in Eq. (8), $w(\mathbf{X}\rightarrow\mathbf{X}+\epsilon_{ik})$ factorizes into two functions $w_1(x_i)$ and $w_2(x_k)$. As a consequence, the steady-state solutions of (7) are easily found:

$$\frac{w_1(x_1)}{w_2(x_1)}=\frac{w_1(x_2)}{w_2(x_2)}=\cdots=\frac{w_1(x_4)}{w_2(x_4)} \qquad (11)$$

which, taking the logarithm, is equivalent to (4).

In the presence of forced exchanges, e.g., ballistic jumps under irradiation, the total jump frequency becomes the sum of the thermal and the athermal frequencies, if those processes act independently:

$$\Gamma_{ik}(\mathbf{X})=\Gamma^{\rm th}_{ik}(\mathbf{X})+\Gamma^{\rm ball} , \qquad (12)$$

where the ballistic jump frequency does not depend on the state of order of the alloy. To take into account the radiation-enhanced thermal mobility (resulting from radiation-sustained point-defect supersaturation), we set, following Ref. 8,

$$\gamma=\frac{\Gamma^{\rm ball}}{\Gamma^{\rm th}_0}=\frac{\Gamma^{\rm ball}}{\Gamma^{\rm th}_0}\exp\left[\frac{E^m_v}{2kT}\right]=\gamma_0\exp\left[\frac{E^m_v}{2kT}\right] , \qquad (13)$$

where $\Gamma^{\rm th}_0$ denotes the enhanced-thermal-jump rate under radiation due to vacancy supersaturation, E^m_v the vacancy migration energy, thus obtaining a temperature-independent quantity γ_0 to measure the external forcing. Inserting the above expressions into (8), we obtain, as final expression for the transition rates,

$$w(\mathbf{X}\rightarrow\mathbf{X}+\epsilon_{ik})=\frac{z}{3}\Gamma_0 x_i(1-x_k)\times\left\{\exp\left[-\frac{2\omega}{kT}\left[(x_i-x_k)+\frac{\omega_0}{\omega}(1-x_i-x_k)\right]\right]+\gamma\right\} , \qquad (14)$$

where we absorbed a factor $\exp(2E_0/kT)$ in Γ_0.

The deterministic equations of motion (7) yield, with expression (14), the kinetics of evolution of the system under nonequilibrium conditions. The attractors of this motion are stable or metastable nonequilibrium steady states, the repellors are unstable states,[9-11] so if there is a single attractor we know the stable phase of the alloy.

Numerical integration for a range of parameter values as well as visual inspection of flow charts of Eq. (7) show the following: for values $\omega_0\geq 0$, only two steady states are possible, one corresponding to the disordered, the other to the $L1_2$-ordered structure, and for negative values of ω_0 we find a range of γ_0 values with a more complicated behavior—at given γ_0 and increasing temperature, the system is first disordered, then orders in an

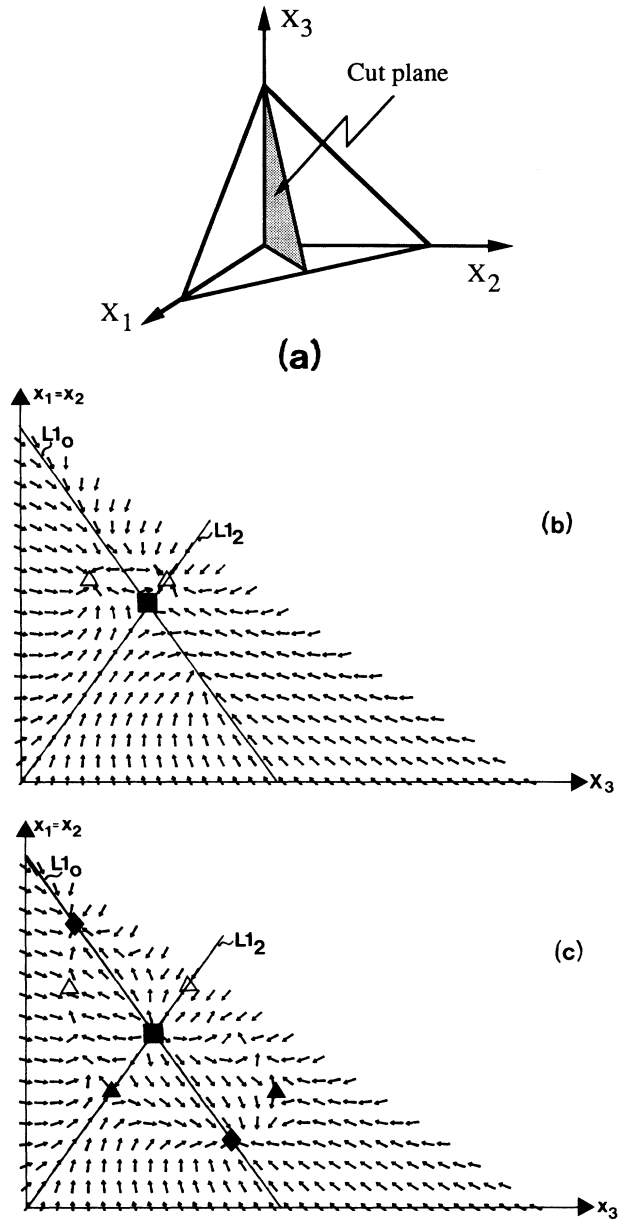

FIG. 2. Two-dimensional cross section of the flow field of the kinetic equation (7) for $\omega_0=-0.5\omega$, $\gamma_0=10^{-6}$ (the length of the arrows is arbitrary). (a) geometry of the cut plane in the three-dimensional order-parameter space [the fourth dimension results from the constraint Eq. (3)]. One variant of the structures of type $L1_2$ and $L1_0$ lies on straight lines in this plane. (b) flow field for $T=0.365T_c$ showing the stability of the $L1^*_2$ phase. (c) flow field for $T=0.370T_c$ showing the stability of the $L1_0$ phase. The points corresponding to the different structures are marked with the following symbols: ■, disorder; ▲, $L1_2$; △, $L1^*_2$; ♦, $L1_0$.

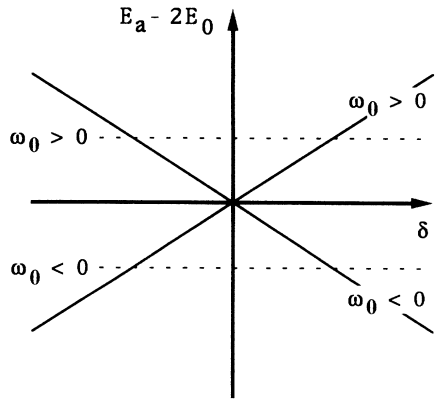

FIG. 3. Schematic plot of the order-parameter dependence of the saddle-point energy E_a for positive and negative values of the saddle-point parameter ω_0 (dashed line, $L1_0$, solid line, $L1_2$).

antiordered $L1_2$ structure (that means preferential occupation of three sublattices, depletion of the fourth, $x_1=x_2=x_3>\frac{1}{4}$, $x_4<\frac{1}{4}$), in the following sometimes denoted $L1_2^*$, then switches to an $L1_0$ structure ($x_1=x_2>\frac{1}{4}$, $x_3=x_4<\frac{1}{4}$), and finally to the true $L1_2$ structure ($x_1=x_2=x_3<\frac{1}{4}$, $x_4>\frac{1}{4}$). For still higher temperatures the systems transform directly back to disorder. As an example for this behavior, the flow chart of Eq. (7) for two different temperatures is shown in Fig. (2). For the numerical calculations, the vacancy migration energy E_v^m was set to the typical value $E_v^m=1$ eV, the equilibrium critical temperature of the $L1_2$ phase (which scales ω) to $T_c=1000$ K.

Qualitatively, the influence of the saddle-point parameter can be understood as follows: from (14) we see that, for $L1_2$-type ordering ($x_1=x_2=x_3=\delta/3$, $x_4=1-\delta$), the activation energy for jumps enhancing this type of order lowers with $\delta\to 0$ for $\omega_0>0$, whereas it rises for $\omega_0<0$ (see Fig. 3). That means that transitions enhancing the order become less favorable with the rising degree of order in the case of $\omega_0<0$. For the $L1_2^*$ structure, this behavior is inversed since the jumps decreasing the $L1_2$ order increase the $L1_2^*$ order.

The $L1_0$ structure ($x_1=x_2=\frac{1}{2}-\delta$, $x_3=x_4=\delta$) does not show this dependence, but generally, the kinetic is enhanced by negative values of ω_0. So under nonequilibrium conditions, even thermodynamically unfavorable structures may be stabilized just by their kinetic behavior.

Another important feature of the numerical investigation of equation (7) is that neither the tetragonal ($x_1=x_2\neq x_3\neq x_4$) nor the orthorhombic ($x_1\neq x_2\neq x_3\neq x_4$) phases have been found to be steady states. Also not found, while possible in principle, were attractors more complicated than simple nodes, e.g. limit cycles.

IV. STABILITY OF COMPETING PHASES

Whenever the kinetic equations exhibit more than one locally stable steady-state solution (first order transition), the above model gives no means to assess the relative stability of the corresponding solution: a knowledge of the steady-state probability of $\mathbf{X}$, $P(\mathbf{X})$ is required. For thermal systems $P(\mathbf{X})$ is

$$P(\mathbf{X})=\frac{1}{Z}\exp\left[-\frac{F(\mathbf{X})}{kT}\right], \tag{15}$$

where Z denotes the configuration sum.

For nonequilibrium systems, the counterpart to the free energy $F(\mathbf{X})$ is *a priori* not known but can be computed if $P(\mathbf{X})$ is known: $P(\mathbf{X})$ can indeed by found from a microscopic model. If we assume, as in Sec. III, that the system is Markovian, i.e., does not possess any memory effects, the probability $P(\mathbf{X},t)$ to find a certain configuration $\mathbf{X}$ at time t is given as solution of the following master equation:

$$\frac{\partial}{\partial t}P(\mathbf{X},t)=\Omega\sum_{\mathbf{X}'}[P(\mathbf{X}',t)w(\mathbf{X}'\to\mathbf{X}) - P(\mathbf{X},t)w(\mathbf{X}\to\mathbf{X}')] . \tag{16}$$

$\mathbf{X}'$ represents the states accessible from $\mathbf{X}$ and the transition rates between $\mathbf{X}$ and $\mathbf{X}'$ are Ω times those given by Eq. (14).

However, even for the stationary case

$$\frac{\partial}{\partial t}P^*(\mathbf{X},t)=0 , \tag{17}$$

a solution of (16) can only be found for special cases, in particular if the condition of detailed balance

$$P^*(\mathbf{X}')w(\mathbf{X}'\to\mathbf{X})=P^*(\mathbf{X})w(\mathbf{X}\to\mathbf{X}') \tag{18}$$

is fulfilled. For nonthermal systems (18) is usually not true but is nevertheless guaranteed for one-dimensional order parameters with single-step kinetics.[12] This property was used in Ref. 3. If (18) is not fulfilled, a common procedure is to transform (16) into a Fokker-Planck equation by expanding both $P(\mathbf{X}+\boldsymbol{\epsilon},t)$ and $w(\mathbf{X}+\boldsymbol{\epsilon}\to\mathbf{X})$ about $P(\mathbf{X})$ and $w(\mathbf{X}\to\mathbf{X}+\boldsymbol{\epsilon})$ in powers of $\boldsymbol{\epsilon}$, which is proportional to an inverse power of the system size Ω (Kramers-Moyal expansion)[13] and truncating after the quadratic term. This technique has several shortcomings: already in the one-dimensional case, where the exact solution of (16) is known, the solution of the Fokker-Planck equation for large but finite system sizes does not converge to the exact solution (see the Appendix). In the multidimensional case, already under purely thermal conditions examples can be found where the Fokker-Planck equation does not fulfill the condition of zero-probability flux, which is the counterpart of the condition of detailed balance in the master equation.[14]

The origin for this difficulty stems from the fact that the asymptotic form of $P(\mathbf{X})$ should be

$$P(\mathbf{X})\propto\exp\Omega\varphi(\mathbf{X}) \tag{19}$$

with an intensive quantity φ.[5,11,15,16] This implies that, in the expansion

$$P(\mathbf{X}+\boldsymbol{\epsilon})=\sum_{n=0}^{\infty}\frac{1}{n!}(\boldsymbol{\epsilon}\cdot\nabla)^nP(\mathbf{X}) , \tag{20}$$

each term in the sum contains a contribution of order

$\mathcal{O}(\Omega^0)$ so that the series does not converge.

Instead of the Fokker-Planck approach, we will use a method proposed by Kubo *et al.*[5] and generalized by Suzuki,[15] which avoids the above problems. Expanding $\varphi(\mathbf{X}+\boldsymbol{\epsilon})$ in Eq. (19) and inserting this in the master equation (16) yields Kubo's equation for φ:

$$\frac{\partial}{\partial t}\varphi(\mathbf{X},t)=\sum_{\epsilon} w(\mathbf{X}\rightarrow\mathbf{X}+\boldsymbol{\epsilon})\{\exp[(\boldsymbol{\epsilon}\cdot\nabla)\varphi]-1\}\ , \tag{21}$$

where $\boldsymbol{\epsilon}$ runs over all possible transitions.

With the definition (6) for the $\boldsymbol{\epsilon}$ in our case, Eq. (21) becomes, for the stationary case,

$$0=\sum_{i,k=1}^{4} w_{ik}(\mathbf{X})\left[1-\exp\left[\frac{\partial\varphi}{\partial x_i}-\frac{\partial\varphi}{\partial x_k}\right]\right]\ , \tag{22}$$

where we introduced the abbreviation

$$w_{ik}(\mathbf{X})=w(\mathbf{X}\rightarrow\mathbf{X}+\boldsymbol{\epsilon}_{ik})\ . \tag{23}$$

V. SOLUTION OF KUBO'S EQUATION

In general, Eq. (22) being a nonlinear partial differential equation seems hard to solve. Nevertheless, in special cases symmetry considerations allow us to reduce it to an ordinary differential equation.

As shown in Sec. III, the stable steady-state solutions correspond either to the disordered $L1_2$ or $L1_0$ structures, which can all be described by a one-dimensional order parameter. Their corresponding points in the four-dimensional order-parameter space lie on an axis of particularly high symmetry: for $L1_2$ these are lines of type

$\mathbf{X}_{L1_2}$:

$$\mathbf{X}=\tfrac{1}{4}[(1,1,1,1)-\lambda(-3,1,1,1)],\quad -\tfrac{1}{3}\le\lambda\le 1 \tag{24}$$

and for $L1_0$

$\mathbf{X}_{L1_0}$:

$$\mathbf{X}=\tfrac{1}{4}[(1,1,1,1)-\mu(1,1,-1,-1)],\quad -1\le\mu\le 1\ . \tag{25}$$

Both can be regarded as intersections of two hyperplanes of type $x_1=x_k$ and the hyperplane given by the constraint (3). Since the four sublattices are strictly equivalent, these hyperplanes are symmetry planes of the order-parameter space and thus also symmetry planes of $\varphi(\mathbf{X})$: the directional derivatives of φ perpendicular to these hyperplanes must vanish.

A. The $L1_2$ structure

One variant of the $L1_2$ structure is located on the intersection of the hyperplanes $x_2=x_3$, $x_3=x_4$, $x_1+x_2+x_3+x_4=1$. Choosing an orthogonal coordinate transformation

$$\mathbf{X}'=\underline{A}(\mathbf{X}-\mathbf{b}) \tag{26}$$

with

$$\underline{A}=\begin{pmatrix} \frac{1}{2} & \frac{1}{2} & \frac{1}{2} & \frac{1}{2} \\ 0 & -\frac{1}{\sqrt{2}} & \frac{1}{\sqrt{2}} & 0 \\ 0 & \frac{1}{\sqrt{6}} & \frac{1}{\sqrt{6}} & -\frac{2}{\sqrt{6}} \\ \frac{\sqrt{3}}{2} & -\frac{1}{2\sqrt{3}} & -\frac{1}{2\sqrt{3}} & -\frac{1}{2\sqrt{3}} \end{pmatrix},\quad \mathbf{b}=\frac{1}{4}\begin{pmatrix}1\\1\\1\\1\end{pmatrix}, \tag{27}$$

all derivatives of $\varphi(\mathbf{X})$ except $\partial\varphi/\partial x_4'$ vanish on this line. Inserting this in Kubo's equation, (22) simplifies to

$$0=w_{12}(\mathbf{X}')\left[\exp\frac{2}{\sqrt{3}}\frac{\partial\varphi}{\partial x_4'}-1\right]+w_{21}(\mathbf{X}')\left[\exp-\frac{2}{\sqrt{3}}\frac{\partial\varphi}{\partial x_4'}-1\right] \tag{28}$$

with the solution

$$\varphi_{L1_2}\left[x_1'=0,x_2'=0,x_3'=0,x_4'=\frac{\sqrt{3}}{2}\xi\right]=\tfrac{3}{4}\int_0^{\xi}\ln\frac{w_{21}\left[x_1'=0,x_2'=0,x_3'=0,x_4'=\frac{\sqrt{3}}{2}\xi'\right]}{w_{12}\left[x_1'=0,x_2'=0,x_3'=0,x_4'=\frac{\sqrt{3}}{2}\xi'\right]}d\xi'$$

$$=\int_0^{\xi}\ln\left\{\frac{(1-\xi')^2}{(1+3\xi')\left[1+\frac{\xi'}{3}\right]}\frac{\exp\left[\frac{2\omega}{kT}\left[\xi'-\frac{\omega_0}{2\omega}(1-\xi')\right]\right]+\gamma}{\exp\left[-\frac{2\omega}{kT}\left[\xi'+\frac{\omega_0}{2\omega}(1-\xi')\right]\right]+\gamma}\right\}d\xi'\ . \tag{29}$$

As shown in the Appendix, this result is identical up to terms of order $\mathcal{O}(\Omega^{-1})$ to that obtained by direct solution of the one-dimensional master equation.

B. The $L1_0$ structure

The $L1_0$-type structures are located on lines $x_1=x_2$, $x_3=x_4$, $x_1+x_2+x_3+x_4=1$. Choosing as rotation matrix in (26),

$$\underline{A}=\begin{pmatrix} \frac{1}{2} & \frac{1}{2} & \frac{1}{2} & \frac{1}{2} \\ \frac{1}{\sqrt{2}} & -\frac{1}{\sqrt{2}} & 0 & 0 \\ 0 & 0 & \frac{1}{\sqrt{2}} & -\frac{1}{\sqrt{2}} \\ \frac{1}{2} & \frac{1}{2} & -\frac{1}{2} & -\frac{1}{2} \end{pmatrix}, \tag{30}$$

we find for (22)

$$0=w_{13}(\mathbf{X}')\left[\exp\frac{\partial\varphi}{\partial x_4'}-1\right]=w_{31}(\mathbf{X}')\left[\exp-\left[\frac{\partial\varphi}{\partial x_4'}-1\right]\right] \tag{31}$$

with the solution

$$\varphi_{L1_0}(x_1'=0,x_2'=0,x_3'=0,x_4'=\tfrac{1}{2}\xi)=\tfrac{3}{4}\int_0^{\xi}\ln\frac{w_{31}(x_1'=0,x_2'=0,x_3'=0,x_4'=\frac{1}{2}\xi')}{w_{13}(x_1'=0,x_2'=0,x_3'=0,x_4'=\frac{1}{2}\xi')}d\xi'$$

$$=\tfrac{1}{2}\int_0^{\xi}\ln\left\{\frac{(1-\xi')\left[1-\frac{\xi'}{3}\right]}{(1+\xi')\left[1+\frac{\xi'}{3}\right]}\frac{\exp\left[\frac{\omega}{kT}\left[\xi'-\frac{\omega_0}{\omega}\right]\right]+\gamma}{\exp\left[-\frac{\omega}{kT}\left[\xi'+\frac{\omega_0}{\omega}\right]\right]+\gamma}\right\}d\xi' . \tag{32}$$

VI. RESULTS

Figure 4 shows an example for the stochastic potential $\varphi(\mathbf{X})$ calculated along the $L1_2$ and $L1_0$ axes for a negative saddle-point parameter ω_0 ($\omega_0=-0.5\omega$) and an intermediate value for the irradiation parameter $\gamma_0=10^{-6}$. For temperatures $T<0.364T_c$, the disordered state is most stable, at about $0.364T_c$ the $L1_2^*$ phase emerges first as metastable then as a stable phase. Then it is passed by the $L1_0$ structure at about $T=0.367T_c$, which itself becomes metastable with respect to the true $L1_2$ structure at $0.380T_c$. Figure 5 shows the phase diagram, i.e., the regime of stability of the respective phases in the (T,γ_0) plane for several values of ω_0. As predicted by the deterministic description, positive values of ω_0 do not change qualitatively the phase diagram, whereas negative values lead to a more complex behavior with new phases between disorder and the thermodynamically stable $L1_2$ phase. These new phases are only found at the low-temperature side around the transition regime, and they are more pronounced for lower values of ω_0.

VII. DISCUSSION AND CONCLUSIONS

The above model shows that, under nonequilibrium conditions, i.e., ballistic jumps acting in parallel with the thermal atomic motion, the phase diagram may change drastically. Phases which, under equilibrium conditions, belong to much higher A concentration can be stabilized. This behavior is similar to that observed in Ni_4Mo,[2,17] where a phase, which is metastable under thermal conditions, can be stabilized by radiation. In Refs. 3 and 4 the influence of cascades, i.e., the simultaneous exchange of more than one pair of atoms, is also discussed, and it is shown that, since the difference in stability of the respective phases is small, the phase diagram may change considerably. Similar effects are to be expected in the present case and deserve further study.

Though in Refs. 3 and 4 the phase diagram for cascade sizes greater than one was calculated with the Fokker-Planck approximation, it turns out that the numerical results of a treatment with Kubo's equation differ only very slightly from the former.[18]

More important changes are to be expected if one departs from the AB_3 stoichiometry. Already in the thermal case, a tetragonal phase (sometimes called L') with $x_1=x_2\neq x_3\neq x_4$ is found.[6] This phase must be described with a two-dimensional order parameter and it is not located on a symmetry axis, so that Kubo's equation cannot be reduced to an ordinary differential equation. However, at least in the thermal case, the transition between the $L1_0$ and the L' phase is of second order. If this still holds under nonequilibrium conditions, the transition can be detected from the curvature of φ at the extremum on the $L1_0$ axis in the direction perpendicular to this axis. The curvature of φ can be found by

differentiating (22). The order of the transition can be deduced from the flow chart of the deterministic model. More general cases, where the steady-state structures would not correspond to any symmetry element, cannot be excluded: a full numerical solution of Kubo's equation would then be unavoidable. Even in the simple cases here, several unexpected features have been revealed: the sensitivity of the phase diagram to the model for the saddle-point energy, the stabilization of strongly nonstoichiometric phases, and the possible occurrence of reentrant regions in the phase diagram.

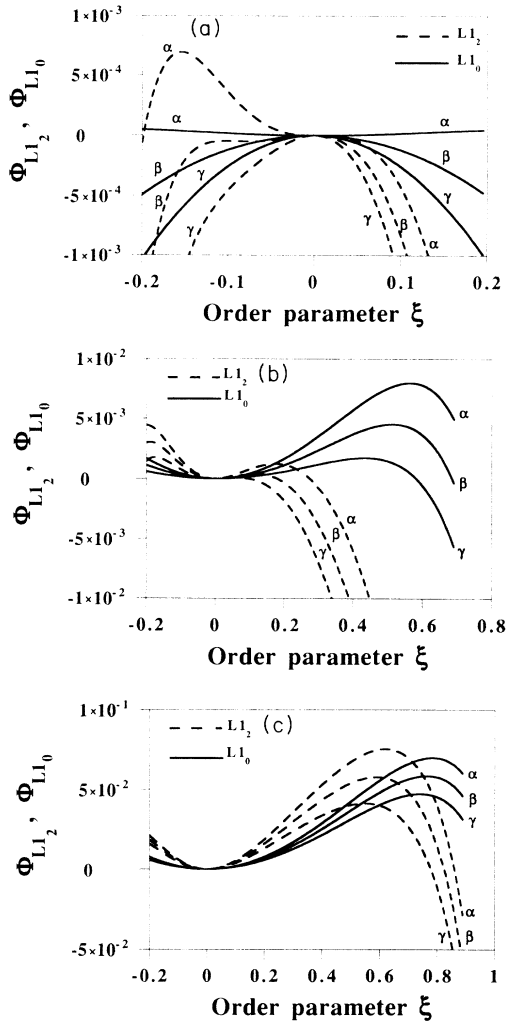

FIG. 4. The stochastic potential φ for the $L1_0$ structure (solid line) and the $L1_2$ structure (dashed line) for $\omega_0=-0.5\omega$, $\gamma_0=10^{-6}$, plotted against the order parameter ξ, showing the stability of the different phases. Both φ and ξ are dimensionless quantities. (a) γ: $T=0.363T_c$, only the disordered phase is stable; β: $T=0.364T_c$, the $L1_2^*$ phase emerges; α: $T=0.365T_c$, the $L1_2^*$ phase becomes more stable than the disordered one. (b) γ: $T=0.366T_c$, the $L1_0$ phase emerges; β: $T=0.367T_c$; γ: $T=0.368T_c$, the $L1_0$ phase becomes the most stable, the $L1_2$ phase emerges. (c) γ: $T=0.376T_c$; β: $T=0.378T_c$; α: $T=0.380T_c$, the $L1_2$ phase becomes the most stable one.

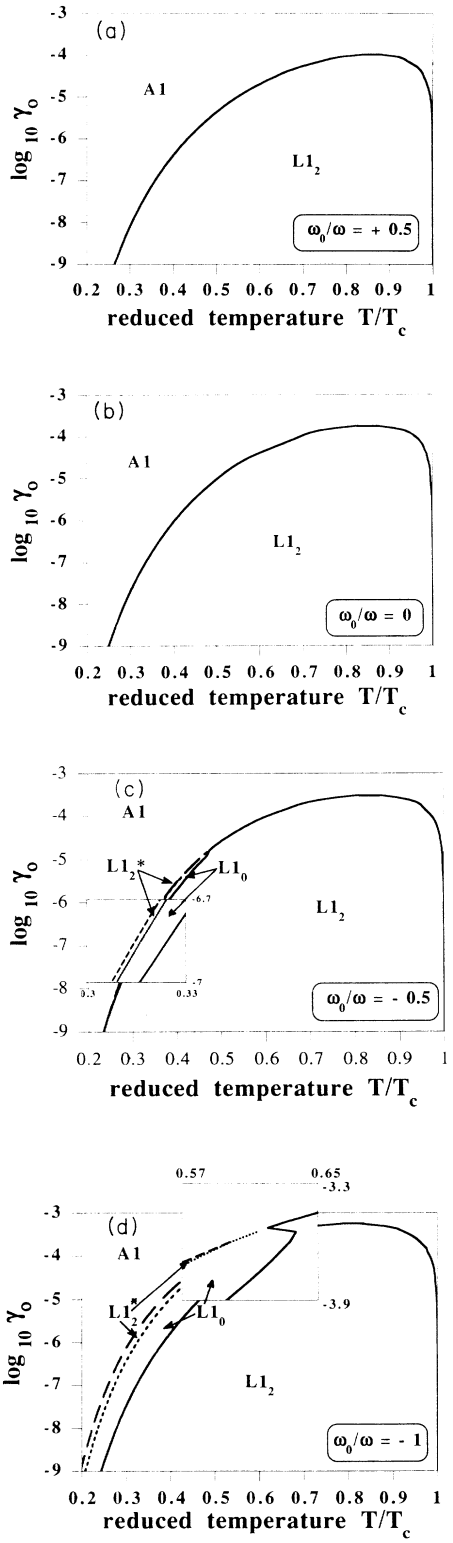

FIG. 5. The dynamic phase diagram in the (T,γ_0) plane for different values of ω_0. T is given in units of the equilibrium critical temperature of the $L1_2$ phase $T_c=1000$ K, γ_0 is dimensionless. (a) $\omega_0=0.5\omega$. (b) $\omega_0=0$. (c) $\omega_0=-0.5\omega$, the inset shows an enlargement of the transition regime. (d) $\omega_0=-1.0\omega$, the inset shows an enlargement of the end of the $L1_0$ and the $L1_2$ existence regime with the reentrant portion of the $L1_2$ phase.

ACKNOWLEDGMENTS

F.H. gratefully acknowledges partial support of this work by a Deutscher Akademischer Austauschdient e.V.-North Atlantic Treaty Organization (DAAD-NATO) grant and a Deutsche Forschungsgemeinschaft (DFG) grant and thanks the members of the Section de Recherches de Métallurgie Physique (SRMP) for their hospitality during his stay at the CEN Saclay.

APPENDIX: COMPARISON OF MASTER EQUATION, FOKKER-PLANCK EQUATION AND KUBO'S EQUATION IN THE ONE-DIMENSIONAL CASE

With N the number of A atoms on sublattice 1, the one-dimensional master equation (ME) reads, under steady-state conditions,

$$-P(N)[W(N\to N+1)+W(N\to N-1)] +P(N+1)W(N+1\to N) +P(N-1)W(N-1\to N)=0 . \quad \text{(A1)}$$

For reflecting boundary conditions, the detailed balance holds even for the nonthermal system:[19]

$$P(N)W(N\to N+1)=P(N+1)W(N+1\to N) , \quad \text{(A2)}$$

so iteration yields

$$\frac{P_{\rm ME}(N)}{P\left[\frac{\Omega}{4}\right]}=\prod_{i=\frac{\Omega}{4}}^{N-1}\frac{W(i\to i+1)}{W(i+1\to i)} =\exp\sum_{i=\frac{\Omega}{4}}^{N-1}\ln\frac{W(i\to i+1)}{W(i+1\to i)} =\exp\Omega\left[\int_{1/4}^{\xi}\ln\frac{w^+(\xi')}{w^-(\xi')}d\xi'+\mathcal{O}(\Omega^{-1})\right] , \quad \text{(A3)}$$

where we put

$$\xi=\frac{N}{\Omega} ,$$

$$w^+(\xi)=\frac{1}{\Omega}W(N\to N+1) \quad \text{(A4)}$$

and

$$w^-(\xi)=\frac{1}{\Omega}W(N\to N-1) .$$

The corresponding Fokker-Planck (FP) equation, obtained by a truncation of the Kramers-Moyal expansion, reads

$$0=\frac{1}{\Omega}\frac{\partial}{\partial\xi}\left[P_{\rm FP}(\xi)[w^+(\xi)-w^-(\xi)] -\frac{1}{2\Omega}\frac{\partial}{\partial\xi}P_{\rm FP}(\xi)[w^+(\xi)+w^-(\xi)]\right] \quad \text{(A5)}$$

with the solution

$$\frac{P_{\rm FP}(\xi)}{P\left[\frac{\Omega}{4}\right]}=\exp 2\Omega\left[\int_{1/4}^{\xi}\frac{w^+(\xi')-w^-(\xi')}{w^+(\xi')+w^-(\xi')}d\xi' +\mathcal{O}\left[\frac{1}{\Omega}\right]\right] . \quad \text{(A6)}$$

Kubo's equation reads

$$0=w^+(\xi)\left[\exp-\frac{\partial\varphi_K}{\partial\xi}-1\right]+w^-(\xi)\left[\exp\frac{\partial\varphi_K}{\partial\xi}-1\right] \quad \text{(A7)}$$

with the solution

$$\varphi_K(\xi)=\int_{1/4}^{\xi}\ln\frac{w^+(\xi')}{w^-(\xi')}d\xi'+\varphi_K(\tfrac{1}{4}) , \quad \text{(A8)}$$

so

$$\frac{P_K(\xi)}{P\left[\frac{\Omega}{4}\right]}=\exp\Omega\int_{1/4}^{\xi}\ln\frac{w^+(\xi')}{w^-(\xi')}d\xi' . \quad \text{(A9)}$$

As expected, (A9) coincides with (A3) up to terms of order $\mathcal{O}(\Omega^{-1})$, whereas (A6) coincides with (A3) only in the region where

$$|w^+-w^-|\ll 1 , \quad \text{(A10)}$$

i.e., in the vicinity of the extrema of P.

*Also at the Section de Recherches de Métallurgie Physique, Centre d'Etudes et de Recherches sur les Materiaux, Centre d'Etudes Nucléaires de Saclay, F-91191 Gif-sur-Yvette CEDEX, France.

[1]K. C. Russell, Prog. Mater. Sci. **28**, 229 (1984).
[2]P. Bellon and G. Martin, Phys. Rev. B **38**, 2570 (1988).
[3]P. Bellon and G. Martin, Phys. Rev. B **39**, 2403 (1989).
[4](a) P. Bellon and G. Martin, J. Less Common Met. **145**, 465 (1988); (b) P. Bellon and G. Martin, Mater. Res. Soc. Symp. Proc. **138**, 15 (1989).
[5]R. Kubo, K. Matsuo, and K. Kithara, J. Stat. Phys. **9**, 51 (1973).
[6]W. Shockley, J. Chem. Phys. **6**, 130 (1938).
[7]L. A. Girifalco, J. Phys. Chem. Solids **24**, 323 (1964).
[8]G. Martin, Phys. Rev. B **30**, 1424 (1984).
[9]R. Görtz, Physica A **90**, 360 (1978).
[10]R. Görtz, Z. Phys. B **36**, 373 (1979).
[11]M. Suzuki, Prog. Theor. Phys. **55**, 383 (1976).
[12]N. G. vanKampen, *Stochastic Processes in Physics and Chemistry* (North-Holland, Amsterdam, 1981).
[13]R. Graham, *Quantum Statistics in Optics and Solid State Physics*, Vol. 66 of *Springer Tracts in Modern Physics*, edited by G. Hohler (Springer, Berlin, 1973).
[14]F. Haider and G. Martin (unpublished).
[15]M. Suzuki, Prog. Theor. Phys. **53**, 1657 (1975).
[16]M. Suzuki, Prog. Theor. Phys. **55**, 1064 (1976).
[17]S. Banerjee, K. Urban, and M. Wilkens, Acta Metall. **32**, 234 (1984).
[18]P. Bellon, F. Haider, and G. Martin, Proceedings of the International Conference on Radiation Material Science, Alushta, 1990 [J. Nucl. Mater. (to be published)].
[19]H. Haken, *Advanced Synergetics* (Springer, Berlin, 1983).

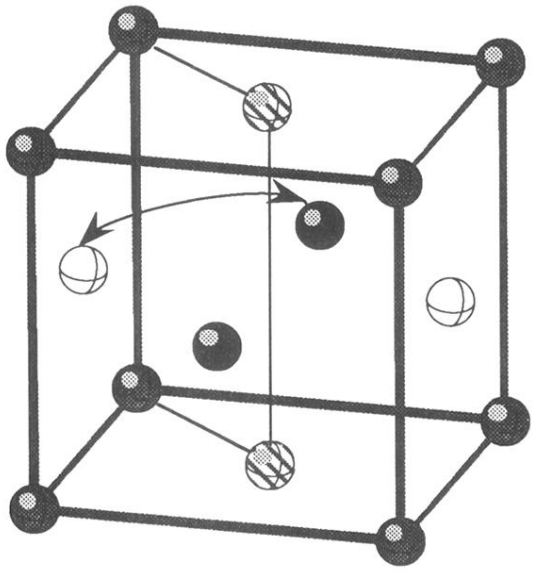

FIG. 1. Unit cell of the fcc lattice showing the four sublattices and the exchange of two neighboring atoms through the "saddle-point window" formed by four atoms.

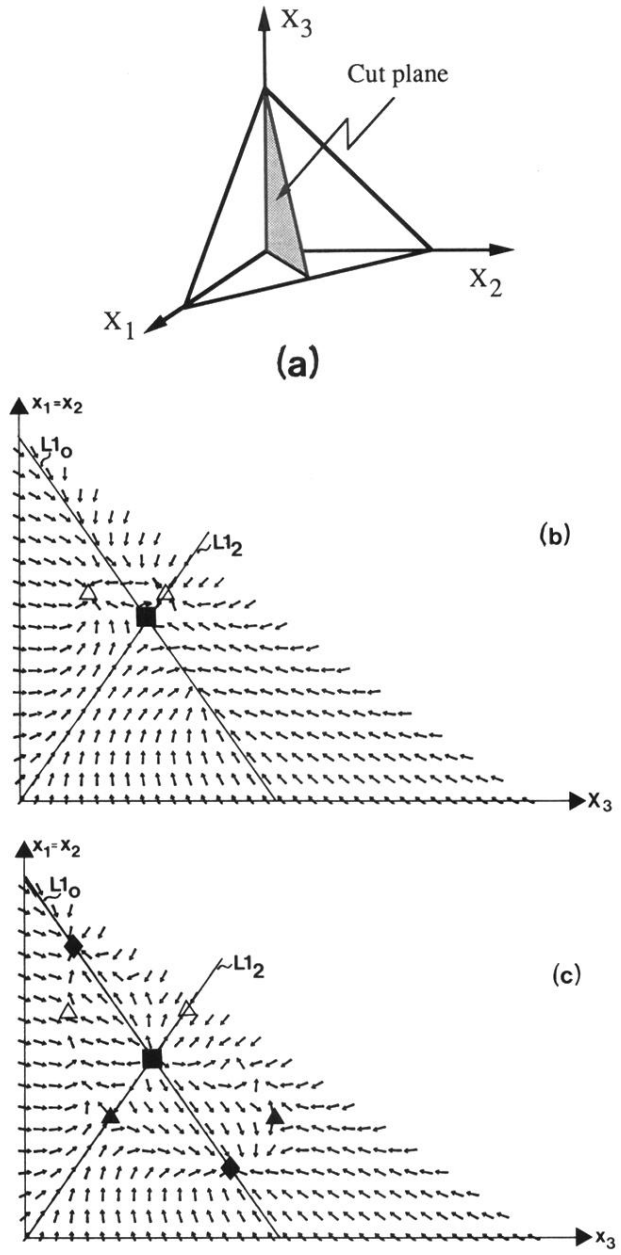

FIG. 2. Two-dimensional cross section of the flow field of the kinetic equation (7) for $\omega_0 = -0.5\omega$, $\gamma_0 = 10^{-6}$ (the length of the arrows is arbitrary). (a) geometry of the cut plane in the three-dimensional order-parameter space [the fourth dimension results from the constraint Eq. (3)]. One variant of the structures of type $L1_2$ and $L1_0$ lies on straight lines in this plane. (b) flow field for $T = 0.365T_c$ showing the stability of the $L1_2^*$ phase. (c) flow field for $T = 0.370T_c$ showing the stability of the $L1_0$ phase. The points corresponding to the different structures are marked with the following symbols: ■, disorder; ▲, $L1_2$; △, $L1_2^*$; ♦, $L1_0$.